JOURNAL OF CHEMICAL INFORMATION AND MODELING

Article

pubs.acs.org/jcim

Discovery of 2-Acylaminothiophene-3-Carboxamides as Multitarget Inhibitors for BCR-ABL Kinase and Microtubules

Ran Cao,[†,‡] Yanli Wang,[‡] and Niu Huang*

National Institute of Biological Sciences, Beijing, No. 7 Science Park Road, Zhongguancun Life Science Park, Beijing, 102206, China

Supporting Information

ABSTRACT: The emergence of drug resistance of the BCR-ABL kinase inhibitor imatinib, especially toward the T315I gatekeeper mutation, poses a great challenge to targeted therapy in treating chronic myeloid leukemia (CML) patients. To discover novel inhibitors against drug-resistant CML bearing T315I mutation, we applied a physics-based hierarchical virtual screening approach to dock a large chemical library against ATP binding pockets of both wild-type (WT) and T315I mutant ABL kinases in a combinatorial fashion. This strategy automatically resulted in 87 compounds satisfying structural and energetic criteria of both WT and T315I mutant kinases. Among them, nine compounds, which share a common thiophene-based scaffold and adopt similar binding poses, were chosen for experimental testing and one of them was shown to have low micromolar inhibition activities against both WT and mutant ABL kinases. Structure−activity relationship analysis with a series of structural modifications based on 2-acylaminothiophene-3-carboxamide scaffold supports our predicted binding mode. Interestingly, the same chemical scaffold was also enriched in our previous virtual screening campaign against colchicine site of microtubules using the same computational protocol, which suggests our virtual screening strategy is capable of discovering small-molecule ligands targeting distinct protein binding sites without sharing any sequential and structural similarity. Furthermore, the multitarget inhibition activity of this class of compounds was assessed in cellular experiments. We expect that the 2-acylaminothiophene-3-carboxamide scaffold may serve as a promising starting point for developing multitarget inhibitors in cancer treatment by targeting both kinases and microtubules.

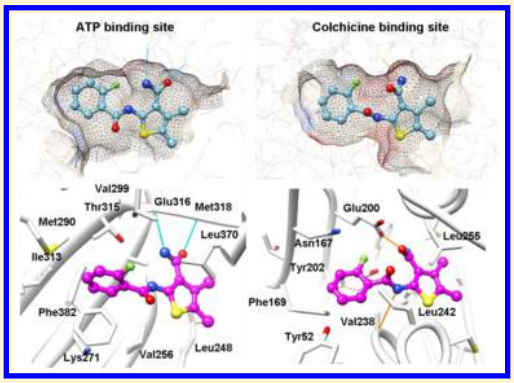

INTRODUCTION

Chronic myelogenous leukemia (CML) is a hematological malignancy resulting from the neoplastic transformation of hematopoietic stem cell.[1] The Philadelphia chromosome (Ph), which accounts for the consistent chromosomal abnormality in CML patients, fuses the Abelson kinase gene (ABL) from chromosome 9 with the breakpoint cluster region (BCR) gene on chromosome 22 and leads to the BCR-ABL protein.[1,2] The resulting BCR-ABL has oncogenic tyrosine kinase activity and promotes cell proliferation and survival, which qualifies it as an important drug target for CML treatment.[1−5]

The first generation BCR-ABL inhibitor imatinib (Chart 1) has achieved great success in the treatment of CML.[6,7] However, a high percentage of clinical relapses has been observed after long-term treatment.[8] Numerous mutations have been revealed to account for the extensive drug resistance, which leads to the development of the second generation BCR-ABL drugs including nilotinib and dasatinib (Chart 1).[9,10] Despite of their effectiveness, a subset of mutants remains resistant. One of them, as exemplified by T315I, represents a great challenge of designing new generation BCR-ABL inhibitors.[11,12]

Based on the ABL-imatinib cocrystal complex structure, it has been hypothesized that the mutation of gatekeeper residue from Thr to Ile obstructs drug binding due to the steric hindrance (Supporting Figure S1A). Thus, new generation inhibitors such as VX-680/PHA-739358 (Supporting Figure S1B), AP24534 (Supporting Figure S1C), and DCC-2036 (Supporting Figure S1D), have been designed to avoid the steric clashes with the T315I gatekeeper mutant. Among them, AP24534 (ponatinib) was approved by FDA as the third generation of BCR-ABL drug despite the potential risk of life-threatening blood clots and severe narrowing of blood vessels.[13] Nevertheless, there's still unmet medical need to explore new chemical scaffold for the development of new generation BCR-ABL drugs.

Physics-based docking and scoring methods have been widely used to identify novel lead compounds.[14] In previous studies, we have reported structure-based hierarchical virtual screening strategies, which integrate different computational approaches in a hierarchical way based on complexity and physically realistic manner in order to strike the balance between efficiency and accuracy.[15,16] We have successfully applied such strategies to identifying novel inhibitors against different drug targets.[16−20] Here, we attempted to discover

Received: May 14, 2015
Published: October 26, 2015

ACS Publications © 2015 American Chemical Society

DOI: 10.1021/acs.jcim.5b00540
J. Chem. Inf. Model. 2015, 55, 2435−2442

Chart 1. Chemical Structures of BCR-ABL Kinase Inhibitors

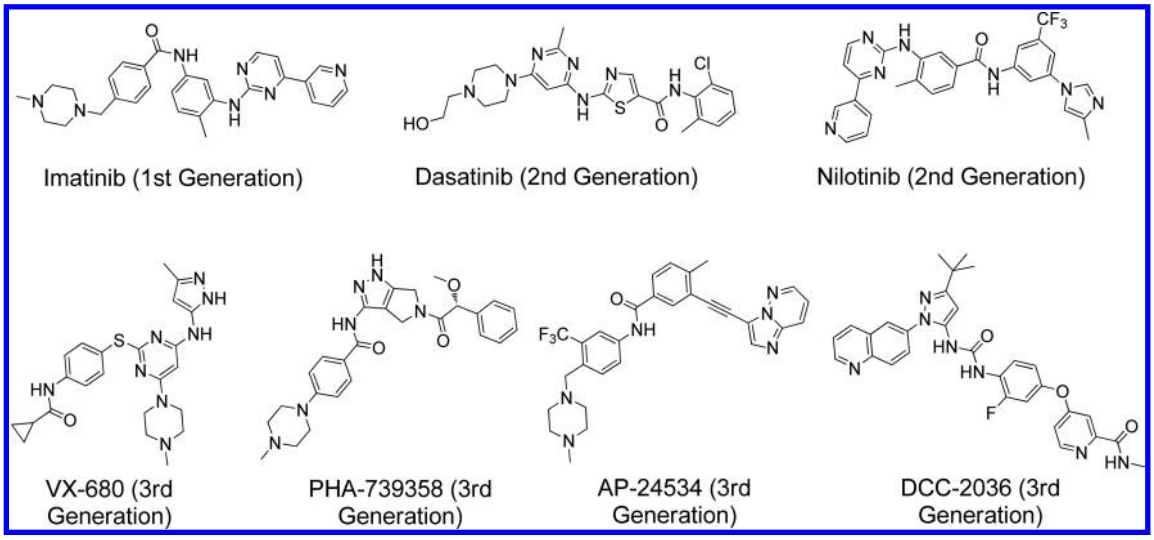

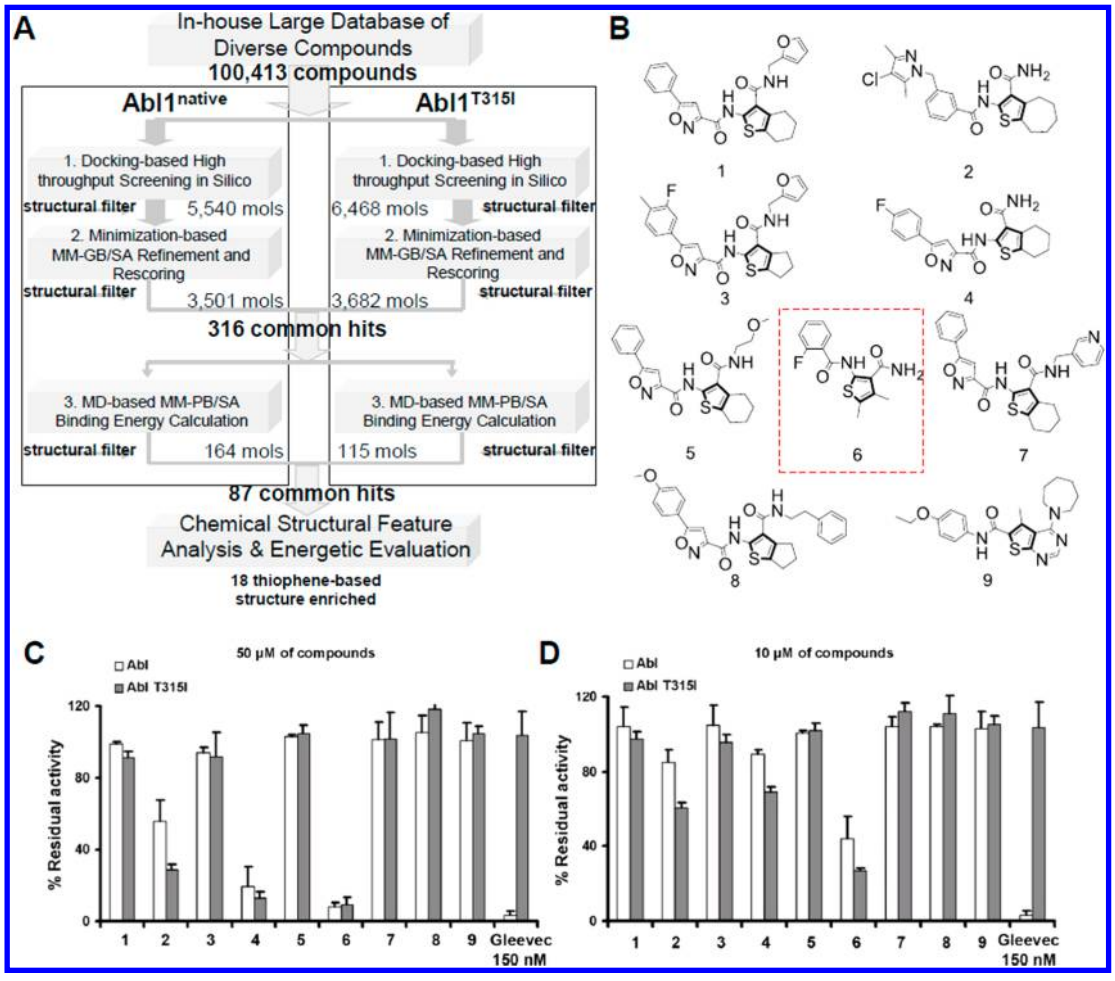

Figure 1. (A) Flowchart of hierarchical virtual screening in a combinatorial strategy against both WT and T315I mutant ABL kinases. (B) Chemical structure of nine representive candidates bearing thiophene core. Kinase inhibitions were measured at concentrations of (C) 50 and (D) 10 μM.

multitarget ligands by applying such an approach in a combinatorial manner against different protein targets, for example, WT and T315I mutant ABL. Surprisingly, we found that the most promising candidate not only shows dual inhibition against ABL WT and mutant kinases but also binds microtubules, a completely different family of cancer targets.

RESULTS AND DISCUSSION

Computational Modeling. For ABL kinase, there are two alternative conformations of the DFG motif, DFG-in and DFG-out, which are referred to as active and inactive conformation, respectively. Targeting the inactive conformation provides considerable selectivity but may suffer much more resist-

DOI: 10.1021/acs.jcim.5b00540
J. Chem. Inf. Model. 2015, 55, 2435−2442

ance.[21,22] In present study, we selected the active conformation of ABL kinase in complex with bosutinib as the starting model (Supporting Figure S2). Herein, we defined two structural filters to remove the unqualified docking poses and docking hits after each step of computational ranking and scoring: (1) the qualified ligands shall form at least one hydrogen bond with the hinge region, including the carbonyl oxygen atom of Glu316 and the amide nitrogen atom of Met318 and (2) the desired candidates shall form close contacts with the residues in the back pocket consisting of Lys271, Met290, Ile313, T315, and Ala380.

Virtual Screening against WT and T315I Mutant. To explore inhibitors against both WT and mutant ABL kinases, we applied structure-based hierarchical virtual screening in a combinatorial manner (Figure 1A). For each target, we conducted molecular docking and MM-GB/SA rescoring by following our previously reported protocol.[16] The top scored hits from both targets were combined and the common hits were selected. Subsequently, MD-PB/SA calculations were performed for these common hits against either target independently. Notably, during each step we applied the structural filters to exclude undesired binding poses. Thus, 5540 and 6468 top scored compounds were selected in docking screenings against WT and T315I mutant, respectively. After MM-GB/SA refining and rescoring, the numbers of the compounds were reduced to 3501 and 3682 with 316 compounds in common. The rest of the compounds were rejected either by their unfavorable MM-GB/SA energy scores (above 0 kcal/mol) or by their minimized binding poses dissatisfying the predefined structural filters. Similarly, MD-PB/SA calculations along with structural filtering resulted in 87 common hits, with a highly enriched thiphene scaffold. Since the same structural scaffold was also enriched in our previous work of discovering antitubulin inhibitors using the same virtual screening protocol;[16] thus, we hypothesized that it is likely to identify lead compounds which are capable of targeting kinases and microtubules simultaneously.

Kinase Inhibition Activities. We chose nine representative compounds with favorable energy scores and containing the common thiophene scaffold (Figure 1B). Initial kinase activity assay was conducted for each compound at concentrations at 50 and 10 μM using imatinib as a positive control. Three out of nine candidates showed strong inhibition against both WT and T315I mutant at 50 μM (Figure 1C). Among these three active compounds, compound **6** was shown inhibition potency at lower concentration of 10 μM (Figure 1D). We further measured the dose response behaviors, and compound **6** showed equivalent potent inhibition of WT and T315I mutant with IC_{50} of 4.0 ± 1.0 and 1.8 ± 0.1 μM, respectively (Figure 2). In contrast, imatinib is inactive against T315I mutant (IC_{50} > 10 μM) comparing to its strong inhibition against WT (IC_{50} = 2.1 ± 0.7 nM), which is consistent with previous reports.[23,24] Interestingly, compound **6** had been discovered in our previous docking screening against tubulin colchicine site, where it was shown to inhibit microtubules assembling in both turbidimetric and sedimentation assays, with a dose-dependent inhibition activity (IC_{50} = 30 ± 5 μM) in turbidimetric assay.[16]

Assessment of Docking Mode. Compound **6** represents a promising structural prototype of multitarget inhibitors against both ABL kinases and microtubules. The ligand binding pose in the context of colchicine site has been systematically probed in our previous study.[16] Here, we further confirmed that compound **6** indeed binds into the colchicine site in

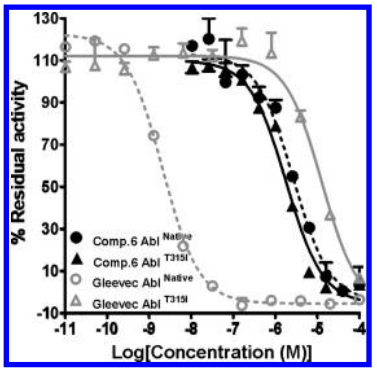

Figure 2. Dose responses of compound **6** and Imatinib in ABL^{WT} and ABL^{T315I} inhibition.

microtubules. According to EBI competitive experiment[25] results (Figure 3), it is found that in the presence of EBI

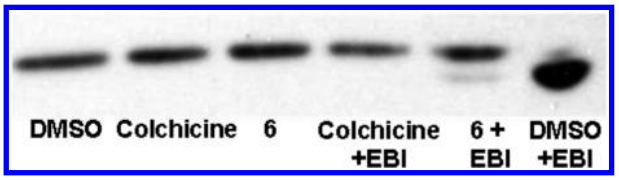

Figure 3. Results of the EBI competitive assay. Compound **6** and colchicine were shown to inhibit the cross-linking of two neighboring cysteines (Cys241 and Cys356) locating at the entrance of colchicine site of tubulin by EBI molecule.

cross-linker, the electrophoresis band of tubulin treated with compound **6** moves at the same speed as with colchicine, both of which was shown slower than DMSO control that represents the fully cross-linked tubulin by EBI. This suggests that compound **6** can effectively inhibit the cross-linking reaction between EBI molecule and the neighboring Cys241 and Cys356 locating at the entrance of colchicine site (Supporting Figure S3), which provides a solid structural basis for our study.

Next, we tested series of structural modifications of compound **6** based on the predicted binding mode (Table 1). The docking modes of compound **6** are almost identical in both WT and T315I mutant ABL structures (Figure 4). Except that the phenyl group of R^1-substituent is more deeply buried into the hydrophobic back pocket, which may lead to the higher affinity of compound **6** toward T315I mutant ABL. More specifically, compound **6** occupies the adenine region by forming two hydrogen bonds with the hinge region and extends into the back pocket behind the gatekeeper residue (Figure 4A). First, we focused on R^1-substituent where the space is relatively enclosed (Figure 4B). Specifically, the ortho-position is pointing outside of the back pocket and allows larger groups. This is validated by the comparable potencies of chlorine- (**6-a**) and bromine-substituents (**6-b**) at this position. In contrast, both meta- and para-positions are located inside the back pocket with close contacts with nonpolar atoms of Lys271, Met290, Val299, Ile313, and Thr315, which is consistent with the reduced inhibition activities of modifications (**6-c**) and (**6-d**) as well as the loss of activity of (**6-e**). Besides, the hydrophobic contacts around R^1 substituent restrict the spacial requirement to planar aromatic ring structures, where the saturated and bulky group (**6-f**) loses activity.

For R^2- and R^3-substituents, the 4,5-dimethyl groups extend outside of the ATP binding pocket with relatively large open

DOI: 10.1021/acs.jcim.5b00540
J. Chem. Inf. Model. 2015, 55, 2435−2442

Table 1. SAR Analysis of Compound 6 in the Context of the ATP Binding Site of ABL^{WT} Kinase

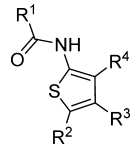

No.	R^1	R^2	R^3	R^4	IC_{50} (μM)	No.	R^1	R^2	R^3	R^4	IC_{50} (μM)
6		Me	Me		4.7	**6-a**		Me	Me		6.1
6-b		Me	Me		1.8	**6-c**	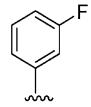	Me	Me		25.8
6-d	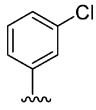	Me	Me		> 50	**6-e**	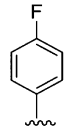	Me	Me		> 50
6-f	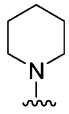	Me	Me		> 50	**6-g**	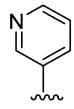	Me	Me		6.7
6-h	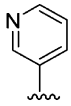	Me	Et		2.3	**6-i**	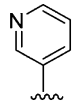	iPr	H		11.0
6-j	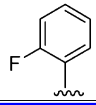	Me	Me		> 50	**6-k**		Me	Me	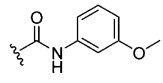	> 50

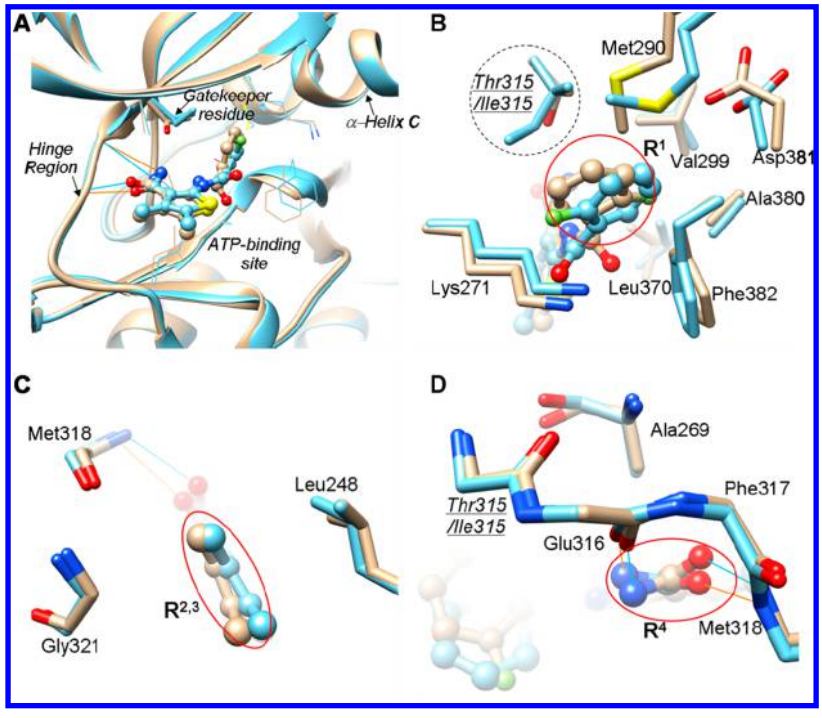

Figure 4. (A) Overall view of predicted binding model of compound **6** (ball and stick) in context of ATP site of WT ABL (ribbon, tan color) and T315I mutant (ribbon, cyan color). (B) Focused view of R^1 group (ball and stick) in the context of the surrounding residues (stick, tan for WT ABL and cyan for T315I mutant). (C) Focused view of R^2 and R^3 groups (ball and stick) in the context of the surrounding residues (stick, tan for WT ABL and cyan for T315I mutant). (D) Focused view of R^4 group (ball and stick) in the context of the surrounding residues (stick, tan for WT ABL and cyan for T315I mutant). Hydrogen bonds are represented in sky blue and orange lines.

DOI: 10.1021/acs.jcim.5b00540
J. Chem. Inf. Model. 2015, 55, 2435−2442

space (Figure 4C). This suggests that the bulky groups could be tolerated, which was confirmed by the activities of ethyl (**6-h**) and propyl substituents (**6-i**). For R^4-substituent, it forms two classical hydrogen bonds with backbone atoms of Glu316 and Met318 in the hinge region (Figure 4D). It is evident that negatively charged group (**6-j**) and bulky group (**6-k**) at this position diminish the activities. Interestingly, a reported JNK3 inhibitor **738** (PDB ID: 2O2U)[26] also contains a thiophene scaffold, and its crystal binding pose in the ATP binding site is highly similar to the docking pose of our identified ABL inhibitors. This may provide an additional support for our docking pose prediction (Supporting Figure S4).

Proliferation Inhibition in Cells. We used parental Ba/F3 cells, WT ABL and T315I mutant ABL driven Ba/F3 cells for our cellular functional testing, which stand for the normal and carcinomatous cell lines, respectively. Compound **6-g** showed significant inhibition against both ABLs driven cell lines in the dose−response fashion while only moderate effect on the parental cells (Figure 5A). This confirms that the *in vitro* inhibition of WT and T315I mutant contributes significantly to the antiproliferation activity of the compound **6-g**. The moderate inhibition of parent Ba/F3 cells may be attributed to the antitubulin potency, as suggested by the EBI cellular experiment results.

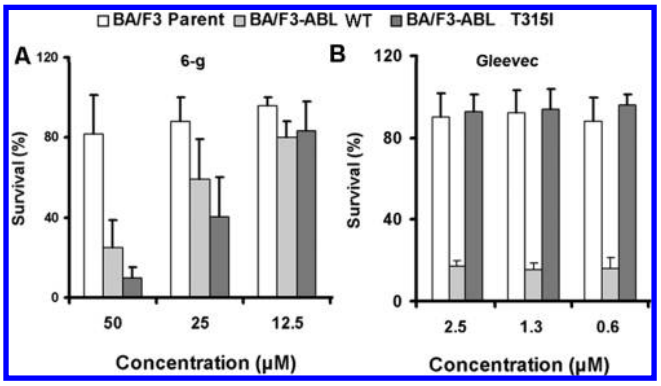

Figure 5. Cell proliferation inhibition in parental, ABL^{wt} driven and ABL^{T315I} driven Ba/F3 cell lines by (A) compound **6-g** and (B) imatinib.

Structural Similarity between the Kinase ATP-Site and Tubulin Colchicine-Site. Compound **6** is a novel multitarget inhibitor against ABL kinases (both WT and T315I mutant forms) and microtubules (Figure 6A and B). Although kinases and microtubules do not share any sequential and structural similarity, the characteristics of the surrounding residues of ligand clearly share common features between ATP binding site in kinases and colchicine binding site in microtubules. Specifically, there are two subpockets in both targets: (1) hydrophobic subpocket I occupied by the 2-(2-fluorobenzamido) moiety of **6**, which consists of Met290, Ile313, Phe382 in ABL kinase (Figure 6C) and includes Phe169, Tyr202, Val238, Leu242 in tubulin (Figure 6D); (2) polar subpocket II occupied by the 3-carboxamide group, which consists of Thr315, Glu316, and Met318 in ABL and includes Glu200 and Tyr202 in tubulin. Besides, the space occupied by the thiophene scaffold is surrounded by hydrophobic residues, including Leu248, Val256, Ala 269, Gly321, and Leu370 in ABL kinase and Leu248, Leu255, Val318, Ala316, and Leu378 in tubulin. Not surprisingly, the above characteristics cannot be revealed by the analysis based on bioinformatics approaches. For example, using SMAP program which relies on the sequence order-independent profile−profile alignment (SOIP-PA),[27] a relatively low raw-score (39.19) and statistically insignificant *P*-value (0.1043) was obtained for these two proteins, indicating a considerable sequential and structural divergence between their binding pockets.

Compound **6** holds promise as antitubulin agent and ABL kinase inhibitor. Wolanin et al. reported that the expression of BCR-ABL can impair mitotic checkpoint and promote resistance to microtubule-targeting agents, including nocoda-

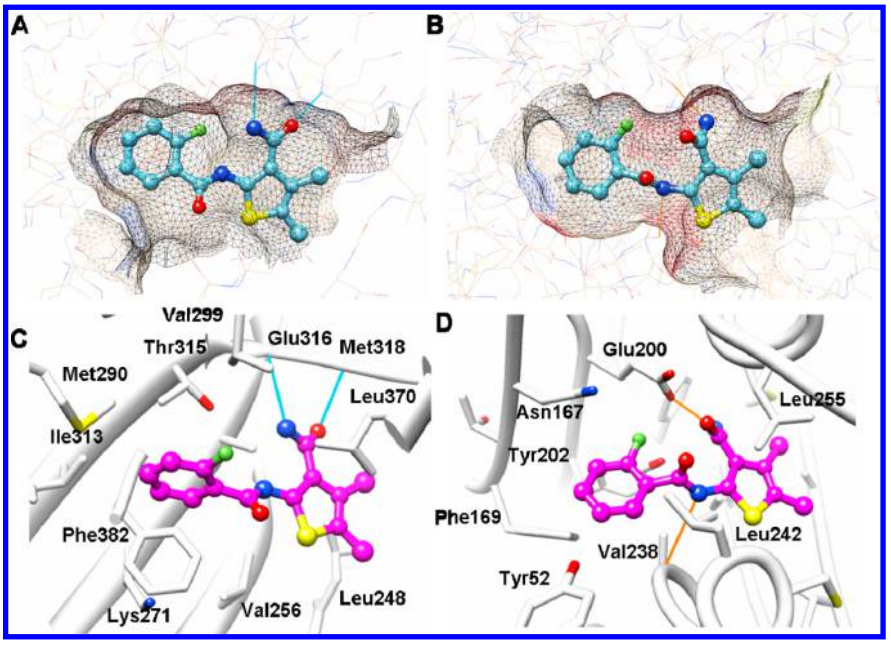

Figure 6. Shape of (A) ATP binding site and (B) colchicine binding site which were defined with residues within 5 Å of compound **6**. Schematic diagram of action mode of compound **6** in context of (C) ATP binding pocket and (D) colchicine binding site. Hydrogen bonds are represented in sky blue and orange lines.

DOI: 10.1021/acs.jcim.5b00540
J. Chem. Inf. Model. 2015, 55, 2435−2442

zole and paclitaxel.[28] It was also found that the inhibition of BCR-ABL with imatinib can enhance the apoptotic efficacy of microtubule-targeting agents in both imatinib sensitive and resistant human CML cells.[29] On this basis, compound **6** provides a promising starting point for the development of multitarget inhibitors in anticancer therapy.

CONCLUSION

In the present study, we applied structure-based hierarchical virtual screening in a combinatorial manner to explore novel lead compounds against both WT and T315I mutant ABL kinases. This strategy automatically results in 18 molecules sharing a common thiophene scaffold. Among nine hits chosen for experimental assays, three compounds, containing 2-acylaminothiophene-3-carboxamide scaffold, were shown potent inhibition against both WT and mutant ABL kinase. Structure−activity relationship study with series of structural modification on this scaffold supported our predicted binding mode. Interestingly, the same structural scaffold was also enriched in our previous docking screening against colchicine site of tubulin using exactly the same computational protocol, which suggests that our parallel virtual screening strategy is capable of discovering small-molecule ligands which target distinct protein binding sites without sharing sequential and structural similarity. On the basis of validated binding pose in the context of both pockets, we proposed that there is ligand-binding similarity between the ATP-site in kinases and colchicine-site in tubulin, which laid the foundation for the development of multitarget inhibitors with a 2-acylaminothiophene-3-carboxamide scaffold against kinases and tubulin.

EXPERIMENTAL SECTION

Chemistry. All the tested compounds were purchased from ChemDiv, ChemBridge, and Vitas M Lab corporations. The vendors had verified the compounds purity by liquid chromatography−mass spectrometry (LC-MS) or nuclear magnetic resonance (NMR) experiments. The ^{1}H NMR spectrum and MS data for lead compound **6** and **6-g** are available in the Supporting Information (Supporting Figure S5−S9).

Computational Details. The crystal structure of ABL in complex with bosutinib (PDB ID: 3UE4) was selected as the starting model. For the T315I mutant, we constructed the gatekeeper mutation by replacing the side chain of Thr315 with Ile315, and then followed with side chain prediction and structural minimization using the Protein Local Optimization Program (PLOP).[15,30−32] Hierarchical virtual screening was conducted according to the previously reported protocol.[16] First, we docked the compound library against target proteins using DOCK 3.5.54.[33−35] As a result, multiple poses were generated for each qualified compound. Second, we carried out MM-GB/SA refinement and rescoring with PLOP. During this process, protein was kept rigid and binding energy was calculated according to $E_{bind} = E^{R*L} - E^{L} - E^{R}$. The highly ranked compounds were further simulated and calculated with MD-based MM-PB/SA method, which was implemented in AMBER10.0 suite.[36] AMBER99SB[37] and general Amber force field (GAFF)[38] were applied for the receptor and ligands, respectively. The AM1-BCC charges calculated with ANTECHAMBER were used for the ligands during the MD-PB/SA calculations. For each complex, three stages of minimization were performed in the gas phase, followed by the addition of a 30 Å water cap based on the geometric center of binding site After 200 ps of equilibration in the solvent, 5 ns production run was performed for the whole system at 300 K with a time step of 2.0 fs, during which all residues (including solvents) beyond 12 Å of ligand were fully frozen. 100 snapshots were evenly extracted from the last 1 ns trajectory and calculated to get the ensemble-average binding energy. Note that we predefined a set of structural filters on the basis of binding characteristics derived from crystal complex structure and available ligand SAR studies, and then filtered out the unqualified docking poses and docking hits after each step of computational ranking and scoring (Figure 1A). All the computational tasks were performed on our internal Linux clusters and managed with the scheduling system SGE.

Expression and Purification of ABL Kinases. The kinase domain of human ABL (residues 229−511, ABL-1a isoform) was studied. The T315I mutant was generated with a one-step overlap extension PCR method by using the Easy Mutagenesis System kit (Transgen). The protein expression and purification were performed as described previously.[39] The purity of the product was checked with SDS-PAGE.

Kinase Activity Assay. ABL (both WT and T315I mutant) kinase assays were performed using the Z′-LYTE Kinase Assay -Tyr 2 Peptide Kit (Invitrogen). Briefly, 0.8 ng WT ABL or 0.5 ng T315I mutant ABL were incubated with compounds at different concentrations for 15 min in 384-well plates with a final volume of 5 μL per well. Reactions were initiated by adding ATP (final concentration: 10 μM) and substrate peptide (final concentration: 2 μM). After incubation for 1 h at the room temperature, reactions were developed and terminated according to the manufacturer's protocol. Then the coumarin and fluorescein emission signals were measured (excitation 400 nm; emission 445 and 520 nm, respectively).

EBI Competitive Assay. BA/F3 and ABL-driven BA/F3 cells were seeded to six well plate (2 × 106 cells per well). Then the cells were treated by 200 μM compound **6-g**, or 40 μM colchicine for 2 h. Subsequently, 100 μM of EBI was added to the cells for 1.5 h at 37 °C without changing the culture medium containing the drug of interest. The control cells were treated with 0.5% DMSO. Afterward, all the cells were harvested and washed with cold PBS buffer. After lysed with 5× SDS loading buffer, the sample was separated with 10% polyacrylamide gel electrophoresis and followed with Western blot analysis. Anti-β-tubulin was purchased from Epitomics, and the peroxidase-conjugated antirabbit immunoglobulin was from Cell Signaling Technology.

Cell Proliferation Inhibition. Parental Ba/F3, Ba/F3 ABL, and Ba/F3 ABL T315I cells were grown in RPMI 1640 supplemented with 10% fetal bovine serum (Life Technologies, Inc.), 1% penicillin G (10,000 units/mL), and streptomycin (10 000 μg/mg) (Life Technologies, Inc.). A 10 ng/mL portion of murin recombinant IL-3 (Prospec Tany, Rehovot, Israel) was added to the growth medium for the parental Ba/F3 cell line. A portion of 20 000 cells/well was added to 96-well plates. Different concentrations of compounds were added and cell proliferation was measured after 48 h using a cell counting kit-8 (Dojindo, Kumamoto, Japan) assay.

Data Analysis and Statistics. All the results were derived from at least three independent experiments. Data were shown as mean values ± SD. Statistical analyses were performed using Student's t test.

DOI: 10.1021/acs.jcim.5b00540
J. Chem. Inf. Model. 2015, 55, 2435−2442

■ ASSOCIATED CONTENT

Supporting Information

The Supporting Information is available free of charge on the ACS Publications website at DOI: 10.1021/acs.jcim.5b00540.

Structure of ABL-bosutinib complex, the results of EBI competitive experiments, the computational results and superposition with crystal structure, as well as the ^{1}H NMR spectrum, MS and HPLC data of the active compounds **6** and **6-g** (PDF)

■ AUTHOR INFORMATION

Corresponding Author

*Phone: 086-1080720645. Fax: 086-1080720813. E-mail: huangniu@nibs.ac.cn.

Present Address

†Institute of Materia Medica, Chinese Academy of Medical Sciences, Peking Union Medical College, No. 1 Xian Nong Tan Street, Beijing, 100050, China.

Author Contributions

‡These authors contributed equally.

Notes

The authors declare no competing financial interest.

■ ACKNOWLEDGMENTS

We thank Prof. John Kuriyan from UC Berkeley for the gift of constructs for ABL kinase. We thank Mr. Zexi Hu and Prof. Liang Chen at NIBS for the gift of Ba/F3 parent cells. We also thank NIBS chemistry center for providing screening library compounds and Dr. Lan Hua for manuscript proofreading. Financial support from the Chinese Ministry of Science and Technology "973" Grant 2014CB849802 (to NH) is gratefully acknowledged. Computational support was provided by the Supercomputing Center of Chinese Academy of Sciences (SCCAS).

■ ABBREVIATIONS

CML, chronic myelogenous leukemia; WT, wild type; MD, molecular dynamics; MM, molecular-mechanics; GB/SA, generalized born surface area; MM-PB/SA, molecular-mechanics Poisson−Boltzmann surface area; PLOP, protein local optimization program

■ REFERENCES

(1) Ren, R. Mechanisms of BCR-ABL in the Pathogenesis of Chronic Myelogenous Leukaemia. *Nat. Rev. Cancer* **2005**, *5*, 172−183.

(2) Savona, M.; Talpaz, M. Getting to the Stem of Chronic Myeloid Leukaemia. *Nat. Rev. Cancer* **2008**, *8*, 341−350.

(3) Frank, D. A.; Varticovski, L. Bcr/Abl leads to the Constitutive Activation of Stat Proteins, and Shares an Epitope with Tyrosine Phosphorylated Stats. *Leukemia* **1996**, *10*, 1724−1730.

(4) Neshat, M. S.; Raitano, A. B.; Wang, H. G.; Reed, J. C.; Sawyers, C. L. The Survival Function of the Bcr-Abl Oncogene is Mediated by Bad-Dependent and -Independent Pathways: Roles for Phosphatidylinositol 3-Kinase and Raf. *Mol. Cell. Biol.* **2000**, *20*, 1179−1186.

(5) Puil, L.; Liu, J.; Gish, G.; Mbamalu, G.; Bowtell, D.; Pelicci, P. G.; Arlinghaus, R.; Pawson, T. Bcr-Abl Oncoproteins Bind Directly to Activators of the Ras Signalling Pathway. *EMBO J.* **1994**, *13*, 764−773.

(6) Frantz, S. Drug Discovery: Playing Dirty. *Nature* **2005**, *437*, 942−943.

(7) Storey, S. Chronic Myelogenous Leukaemia Market. *Nat. Rev. Drug Discovery* **2009**, *8*, 447−448.

(8) Daley, G. Q. Gleevec Resistance: Lessons for Target-Directed Drug Development. *Cell Cycle* **2003**, *2*, 189−190.

(9) Weisberg, E.; Manley, P. W.; Cowan-Jacob, S. W.; Hochhaus, A.; Griffin, J. D. Second Generation Inhibitors of BCR-ABL for the Treatment of Imatinib-Resistant Chronic Myeloid Leukaemia. *Nat. Rev. Cancer* **2007**, *7*, 345−356.

(10) Gorre, M. E.; Mohammed, M.; Ellwood, K.; Hsu, N.; Paquette, R.; Rao, P. N.; Sawyers, C. L. Clinical Resistance to STI-571 Cancer Therapy Caused by BCR-ABL Gene Mutation or Amplification. *Science* **2001**, *293*, 876−880.

(11) Muller, B. A. Imatinib and Its Successors–How Modern Chemistry Has Changed Drug Development. *Curr. Pharm. Des.* **2009**, *15*, 120−133.

(12) Zhang, J.; Adrian, F. J.; Jahnke, W.; Cowan-Jacob, S. W.; Li, A. G.; Iacob, R. E.; Sim, T.; Powers, J.; Dierks, C.; Sun, F.; Guo, G. R.; Ding, Q.; Okram, B.; Choi, Y.; Wojciechowski, A.; Deng, X.; Liu, G.; Fendrich, G.; Strauss, A.; Vajpai, N.; Grzesiek, S.; Tuntland, T.; Liu, Y.; Bursulaya, B.; Azam, M.; Manley, P. W.; Engen, J. R.; Daley, G. Q.; Warmuth, M.; Gray, N. S. Targeting Bcr-Abl by Combining Allosteric with ATP-Binding-Site Inhibitors. *Nature* **2010**, *463*, 501−506.

(13) Pal, A.; Panja, B.; Dutta, T.; Bhowmick, S.; Nath, S.; Bhattacharjee, S. Ponatinib: a Miracle or a Disaster in Chronic Myeloid Leukemia. *Int. J. Basic Clin. Pharmacol.* **2014**, *3*, 933−936.

(14) Huang, N.; Jacobson, M. P. Physics-Based Methods for Studying Protein-Ligand Interactions. *Curr. Opin. Drug Discovery Devel.* **2007**, *10*, 325−331.

(15) Huang, N.; Kalyanaraman, C.; Irwin, J. J.; Jacobson, M. P. Physics-Based Scoring of Protein-Ligand Complexes: Enrichment of Known Inhibitors in Large-Scale Virtual Screening. *J. Chem. Inf. Model.* **2006**, *46*, 243−253.

(16) Cao, R.; Liu, M.; Yin, M.; Liu, Q.; Wang, Y.; Huang, N. Discovery of Novel Tubulin Inhibitors via Structure-Based Hierarchical Virtual Screening. *J. Chem. Inf. Model.* **2012**, *52*, 2730−2740.

(17) Cao, R.; Huang, N.; Wang, Y. Evaluation and Application of MD-PB/SA in Structure-Based Hierarchical Virtual Screening. *J. Chem. Inf. Model.* **2014**, *54*, 1987−1996.

(18) Lin, X.; Huang, X.-P.; Chen, G.; Whaley, R.; Peng, S.; Wang, Y.; Zhang, G.; Wang, S. X.; Wang, S.; Roth, B. L.; Huang, N. Life Beyond Kinases: Structure-Based Discovery of Sorafenib as Nanomolar Antagonist of 5-HT Receptors. *J. Med. Chem.* **2012**, *55*, 5749−5759.

(19) Li, W.; Wan, X.; Zeng, F.; Xie, Y.; Wang, Y.; Zhang, W.; Li, L.; Huang, N. More Than Just a GPCR Ligand: Structure-Based Discovery of Thioridazine Derivatives as Pim-1 Kinase Inhibitors. *MedChemComm* **2014**, *5*, 507−511.

(20) Wan, X.; Zhang, W.; Li, L.; Xie, Y.; Li, W.; Huang, N. A New Target for an Old Drug: Identifying Mitoxantrone as a Nanomolar Inhibitor of PIM1 Kinase via Kinome-Wide Selectivity Modeling. *J. Med. Chem.* **2013**, *56*, 2619−2629.

(21) Huse, M.; Kuriyan, J. The Conformational Plasticity of Protein Kinases. *Cell* **2002**, *109*, 275−282.

(22) Liu, Y.; Gray, N. S. Rational Design of Inhibitors that Bind to Inactive Kinase Conformations. *Nat. Chem. Biol.* **2006**, *2*, 358−364.

(23) Shah, N. P.; Nicoll, J. M.; Nagar, B.; Gorre, M. E.; Paquette, R. L.; Kuriyan, J.; Sawyers, C. L. Multiple BCR-ABL Kinase Domain Mutations Confer Polyclonal Resistance to the Tyrosine Kinase Inhibitor Imatinib (STI571) in Chronic Phase and Blast Crisis Chronic Myeloid Leukemia. *Cancer Cell* **2002**, *2*, 117−125.

(24) Chan, W. W.; Wise, S. C.; Kaufman, M. D.; Ahn, Y. M.; Ensinger, C. L.; Haack, T.; Hood, M. M.; Jones, J.; Lord, J. W.; Lu, W. P.; Miller, D.; Patt, W. C.; Smith, B. D.; Petillo, P. A.; Rutkoski, T. J.; Telikepalli, H.; Vogeti, L.; Yao, T.; Chun, L.; Clark, R.; Evangelista, P.; Gavrilescu, L. C.; Lazarides, K.; Zaleskas, V. M.; Stewart, L. J.; Van Etten, R. A.; Flynn, D. L. Conformational Control Inhibition of the BCR-ABL1 Tyrosine Kinase, Including the Gatekeeper T315I Mutant, by the Switch-Control Inhibitor DCC-2036. *Cancer Cell* **2011**, *19*, 556−568.

(25) Fortin, S.; Lacroix, J.; Cote, M. F.; Moreau, E.; Petitclerc, E.; C.-Gaudreault, R. Quick and Simple Detection Technique to Assess the Binding of Antimicrotubule Agents to the Colchicine-Binding Site. *Biol. Proced. Online* **2010**, *12*, 113−117.

DOI: 10.1021/acs.jcim.5b00540
J. Chem. Inf. Model. 2015, 55, 2435−2442

(26) Angell, R. M.; Atkinson, F. L.; Brown, M. J.; Chuang, T. T.; Christopher, J. A.; Cichy-Knight, M.; Dunn, A. K.; Hightower, K. E.; Malkakorpi, S.; Musgrave, J. R.; Neu, M.; Rowland, P.; Shea, R. L.; Smith, J. L.; Somers, D. O.; Thomas, S. A.; Thompson, G.; Wang, R. N-(3-Cyano-4,5,6,7-tetrahydro-1-benzothien-2-yl)amides as Potent, Selective, Inhibitors of JNK2 and JNK3. *Bioorg. Med. Chem. Lett.* **2007**, *17*, 1296−1301.
(27) Xie, L.; Bourne, P. E. Detecting Evolutionary Relationships across Existing Fold Space, Using Sequence Order-Independent Profile-Profile Alignments. *Proc. Natl. Acad. Sci. U. S. A.* **2008**, *105*, 5441−5446.
(28) Wolanin, K.; Magalska, A.; Kusio-Kobialka, M.; Podszywalow-Bartnicka, P.; Vejda, S.; McKenna, S. L.; Mosieniak, G.; Sikora, E.; Piwocka, K. Expression of Oncogenic Kinase Bcr-Abl Impairs Mitotic Checkpoint and Promotes Aberrant Divisions and Resistance to Microtubule-Targeting Agents. *Mol. Cancer Ther.* **2010**, *9*, 1328−1338.
(29) Greene, L. M.; Kelly, L.; Onnis, V.; Campiani, G.; Lawler, M.; Williams, D. C.; Zisterer, D. M. STI-571 (Imatinib Mesylate) Enhances the Apoptotic Efficacy of Pyrrolo-1,5-benzoxazepine-6, a Novel Microtubule-Targeting Agent, in Both STI-571-Sensitive and -Resistant Bcr-Abl-Positive Human Chronic Myeloid Leukemia Cells. *J. Pharmacol. Exp. Ther.* **2007**, *321*, 288−297.
(30) Jacobson, M. P.; Kaminski, G. A.; Friesner, R. A.; Rapp, C. S. Force Field Validation Using Protein Side Chain Prediction. *J. Phys. Chem. B* **2002**, *106*, 11673−11680.
(31) Jacobson, M. P.; Pincus, D. L.; Rapp, C. S.; Day, T. J.; Honig, B.; Shaw, D. E.; Friesner, R. A. A Hierarchical Approach to All-Atom Protein Loop Prediction. *Proteins: Struct., Funct., Genet.* **2004**, *55*, 351−367.
(32) Li, X.; Jacobson, M. P.; Friesner, R. A. High-Resolution Prediction of Protein Helix Positions and Orientations. *Proteins: Struct., Funct., Genet.* **2004**, *55*, 368−382.
(33) Meng, E. C.; Shoichet, B. K.; Kuntz, I. D. Automated Docking with Grid-Based Energy Evaluation. *J. Comput. Chem.* **1992**, *13*, 505−524.
(34) Lorber, D. M.; Shoichet, B. K. Hierarchical Docking of Databases of Multiple Ligand Conformations. *Curr. Top. Med. Chem.* **2005**, *5*, 739−749.
(35) Wei, B. Q.; Baase, W. A.; Weaver, L. H.; Matthews, B. W.; Shoichet, B. K. A Model Binding Site for Testing Scoring Functions in Molecular Docking. *J. Mol. Biol.* **2002**, *322*, 339−355.
(36) Case, D. A.; Darden, T. A.; Cheatham, I. T. E.; Simmerling, C. L.; Wang, J.; Duke, R. E.; Luo, R.; Crowley, M.; Walker, R. C.; Zhang, W.; Merz, K. M.; Wang, B.; Hayik, S.; Roitberg, A.; Seabra, G.; Kolossváry, I.; Wong, K. F.; Paesani, F.; Vanicek, J.; Wu, X.; Brozell, S. R.; Steinbrecher, T.; Gohlke, H. *AMBER, version 10*. http://ambermd.org/ (accessed August 2010).
(37) Wang, J.; Cieplak, P.; Kollman, P. A. How Well Does a Restrained Electrostatic Potential (RESP) Model Perform in Calculating Conformational Energies of Organic and Biological Molecules? *J. Comput. Chem.* **2000**, *21*, 1049−1074.
(38) Wang, J.; Wolf, R. M.; Caldwell, J. W.; Kollman, P. A.; Case, D. A. Development and Testing of a General Amber Force Field. *J. Comput. Chem.* **2004**, *25*, 1157−1174.
(39) Seeliger, M. A.; Young, M.; Henderson, M. N.; Pellicena, P.; King, D. S.; Falick, A. M.; Kuriyan, J. High Yield Bacterial Expression of Active c-Abl and c-Src Tyrosine Kinases. *Protein Sci.* **2005**, *14*, 3135−3139.

DOI: 10.1021/acs.jcim.5b00540
J. Chem. Inf. Model. 2015, 55, 2435−2442